

Characterizing Polymer Brushes via Surface Wrinkling

Heqing Huang, Jun Young Chung, Adam J. Nolte, and Christopher M. Stafford*

*Polymers Division, National Institute of Standards and Technology, 100 Bureau Drive,
Gaithersburg, Maryland 20899*

Received August 28, 2007. Revised Manuscript Received September 27, 2007

We apply surface wrinkling to measure the mechanical properties of poly(2-hydroxyethyl methacrylate) polymer brush layers tethered to the surface of a flexible poly(dimethylsiloxane) (PDMS) substrate. A facile modification scheme based on hydrochloric acid treatment was employed to introduce hydroxyl groups to the surface of PDMS, which served to covalently attach initiator groups for subsequent polymerization. Upon mechanical compression of the brush layer on PDMS, a wrinkling instability occurs whose wavelength yields a Young's modulus for the brush layer that is comparable to the corresponding polymer in the bulk. Moreover, we show that the wrinkling wavelength can provide an accurate measure of the brush thickness, which is often difficult to assess on transparent, flexible substrates. When using thermal strain to generate wrinkled surfaces, the patterns are stable at room temperature but can be erased by solvent treatment, which relaxes the applied strain and thus imparts reversibility to the wrinkled surfaces.

1. Introduction

In many applications, the surface properties of a material or device play a critical role in the overall performance and reliability. Polymer brushes present a versatile route for modulating specific properties of a surface through tailored brush chemistry and architecture,¹ and they have been utilized to manipulate adhesion and friction,^{2–4} tune biocompatibility,⁵ and tailor the near-surface mechanical properties.⁶ Polymer brushes have also been used as stable intermediates for the immobilization of peptides, DNA, and proteins on the surfaces of microfluidic channels^{7–9} fabricated from poly(dimethylsiloxane) (PDMS). PDMS is a principal candidate in many biomaterial and microfluidic applications due in part to its flexibility, optical clarity, and elastic tunability. Consequently, there is a growing need for facile chemistries capable of introducing reactive groups on the surface of PDMS that do not significantly alter the underlying mechanical properties, given that these properties govern important biological responses such as cell attachment, spreading, and proliferation.^{10–12} An additional challenge is

that it is extremely difficult to measure the mechanical and structural properties of the brush layer attached to a surface, even more so when the brush is on a soft, flexible substrate such as PDMS.

In this paper, we report four key accomplishments: first, we demonstrate the use of hydrochloric acid (HCl) treatment to introduce hydroxyl groups on the surface of PDMS without the formation of a stiff oxide layer; second, we use surface wrinkling to measure the mechanical properties of poly(2-hydroxyethyl methacrylate) (PHEMA) brushes grafted directly from the surface of PDMS; third, we show that surface wrinkling can provide reliable estimates of the brush layer thickness, which can be difficult to assess on transparent, flexible substrates; and last, we illustrate how thermal treatment can produce a wrinkled sample that is stable at room temperature but can be reversibly switched off and on by alternating solvent and thermal treatments. We suggest ways in which such reversibly patterned surfaces could be used for various applications in surface engineering.

2. Experimental Section

2.1. General. All chemicals were obtained from Aldrich and used as received, unless otherwise noted. Water contact angles were measured using a Krüss G2 contact angle measuring system. Equipment and materials are identified in this paper in order to adequately specify the experimental details. Such identification does not imply recommendation by NIST, nor does it imply that the materials are necessarily the best available for the purpose.

2.2. Preparation of Gradient Thickness Polymer Brush Layers on PDMS. PDMS elastomer was prepared by mixing Sylgard 184 (Dow Corning) in a 10:1 ratio by mass of oligomeric base to curing agent and casting against a polished silicon wafer and then curing at 75 °C for 24 h. The thickness of the cured PDMS sheet was 2 mm. The PDMS was cut into 75 mm × 10 mm

* Corresponding author: e-mail chris.stafford@nist.gov.

- (1) Advincula, R. *Adv. Polym. Sci.* **2006**, *197*, 107.
- (2) Wong, J. Y.; Kuhl, T. L.; Israelachvili, J. N.; Mullah, N.; Zalipsky, S. *Science* **1997**, *275*, 820.
- (3) Retsos, H.; Kiriy, A.; Senkovskyy, V.; Stamm, M.; Feldstein, M. M.; Creton, C. *Adv. Mater.* **2006**, *18*, 2624.
- (4) Klein, J.; Kumacheva, E.; Mahalu, D.; Perahla, D.; Fetters, L. J. *Nature (London)* **1994**, *370*, 634.
- (5) Senaratne, W.; Andruzzi, L.; Ober, C. K. *Biomacromolecules* **2005**, *6*, 2427.
- (6) LeMieux, M. C.; Peleshanko, S.; Anderson, K. D.; Tsukruk, V. V. *Langmuir* **2007**, *23*, 265.
- (7) Sui, G. D.; Wang, J. Y.; Lee, C. C.; Lu, W. X.; Lee, S. P.; Leyton, J. V.; Wu, A. M.; Tseng, H.-R. *Anal. Chem.* **2006**, *78*, 5543.
- (8) Hu, S. W.; Ren, X. Q.; Bachman, M.; Sims, C. E.; Li, G. P.; Allbritton, N. *Anal. Chem.* **2002**, *74*, 4117.
- (9) Patrito, N.; McCague, C.; Chiang, S.; Norton, P. R.; Petersen, N. O. *Langmuir* **2006**, *22*, 3453.
- (10) Dutta, A. K.; Belfort, G. *Langmuir* **2007**, *23*, 3088.
- (11) Thompson, M. T.; Berg, M. C.; Tobias, I. S.; Lichter, J. A.; Rubner, M. F.; Van Vliet, K. J. *Biomacromolecules* **2006**, *7*, 1990.

- (12) Mei, Y.; Wu, T.; Xu, C.; Langenbach, K. J.; Elliott, J. T.; Vogt, B. D.; Beers, K. L.; Amis, E. J.; Washburn, N. R. *Langmuir* **2005**, *21*, 12309.

specimens and Soxhlet extracted with toluene for 24 h to remove any un-cross-linked chains. The extracted PDMS slides were immersed in 10 vol % aqueous HCl solution for 16 h, rinsed copiously with deionized (DI) water, and dried under vacuum at room temperature for 1 h. The initiator, 11-(2-bromo-2-methyl)propionyloxyundecyltrichlorosilane, was synthesized as described in the literature.^{3,12} Acid-treated PDMS was then immersed in an initiator solution (1 mmol/L in toluene) for 16 h followed by Soxhlet extraction with toluene for 24 h. As a control, a silicon wafer having the same dimensions as the PDMS was subjected to the initiator immobilization and atom transfer radical polymerization (ATRP) conditions in parallel with the treatments of the PDMS substrates. The initiator-functionalized PDMS was stored under argon less than 48 h before surface-initiated polymerization.

Prior to polymerization, a monomer mixture (6 mL of HEMA and 6 mL of deionized water) was degassed for 2 h and then transferred to a tube containing the degassed catalyst complex (374 mg of 2,2'-bipyridine, 84 mg of CuCl, and 54 mg of CuBr₂). In order to create a discrete thickness gradient of tethered PHEMA chains, the monomer/catalyst solution was pumped stepwise into a degassed test tube containing both a modified PDMS substrate and a reference silicon wafer at an interval of 15 or 25 min per step, depending on the desired thickness of each step. Polymerization proceeded at room temperature and was terminated by exposure of the monomer solution to air. The PHEMA-grafted PDMS (PDMS-*g*-PHEMA) substrate was cleaned with dimethylformamide (DMF) in an ultrasonic bath for 2 min and rinsed copiously with methanol to remove any unreacted monomer. The cleaned PDMS-*g*-PHEMA was then stored in DMF to reduce the possibility of the hydrophobic recovery of PDMS.

2.3. Attenuated Total Reflection FTIR (ATR-FTIR). ATR-FTIR analysis of PDMS-*g*-PHEMA was performed using a Nicolet Nexus 670 spectrometer equipped with a liquid nitrogen-cooled mercury cadmium telluride detector. The spectra were collected over a range of 650–4000 cm⁻¹ with a nominal resolution of 4.0 cm⁻¹ and were averaged over 1024 scans. The acid-treated PDMS specimens were scanned as the background, and a brush-modified PDMS specimen was scanned to verify the presence of PHEMA on the surface.

2.4. Variable Angle Spectroscopic Ellipsometry (VASE). The thickness of PHEMA on PDMS was measured by spectroscopic ellipsometry (M-2000DI, J.A. Woollam Co.) under ambient conditions. The angle of incidence for all measurements ranged from 50° to 70° at an interval of 5°, and the wavelength range was 300 to 1000 nm. The ellipsometric data were fit to determine the thickness of polymer film layer, the exact angle of incidence, and refractive index of the brush layer using a Cauchy dispersion relationship.¹³

2.5. Surface Wrinkling. Prior to wrinkling, the samples were dried in a vacuum oven at 50 °C for 2 h at a relative humidity (RH) of 20% and the Young's modulus of the PDMS substrates was determined on a texture analyzer (model TA.XT2i, Texture Technologies Corp.) in tension mode. In all experiments presented here, the modulus of the PDMS substrate was $E_s = 2.4 \pm 0.1$ MPa as measured by tensile tests, and the poisson's ratio was assumed to be $\nu_s = 0.50$. Wrinkling of the PDMS-*g*-PHEMA brush specimens was achieved through both mechanical compression and thermal cycling. For mechanical compression, a small compressive strain was applied via a pair of tweezers, and photographs of the wrinkled pattern were taken using an optical microscope (Nikon Optiphot) at a magnification of 100×. Thermal wrinkling of the polymer brush layer was achieved by placing the sample in a

convection oven at 100 °C (higher than the T_g of PHEMA^{14,15}) for 20 min and then allowing it to cool to room temperature. Atomic force microscopy (AFM) images (Dimension 3100, Veeco Instruments, operating in tapping mode) and optical microscopy images were taken of the wrinkled surfaces. Fourier image transforms were conducted on each optical micrograph to determine the average wavelength (λ) of the wrinkling pattern. As a reference, a nontethered thin film of PHEMA (molar mass = 300 000 g/mol, Aldrich Inc.) on PDMS was obtained with a 2 wt % PHEMA in ethanol using a flow-coating technique.¹⁶

In addition, the reversibility of the wrinkling process was tested by solvent swelling (water, ethanol, or DMF) of the brush layer to "erase" the wrinkled pattern, followed by thermal wrinkling as described above. This cycle was repeated several times. An optical image was taken at a single position along the gradient after each solvent and thermal treatment.

3. Results and Discussion

3.1. Grafting of PHEMA Brushes from PDMS. Grafting polymer brushes from a surface involves immobilization of initiator moieties on the surface followed by surface-initiated polymerization (ATRP in our case). In the case of grafting from silicon or glass, the surface silanol groups inherent to these materials provide a convenient and reliable route for attaching chlorosilane-based initiators. However, immobilization of initiator groups on the surface of PDMS requires an additional step to introduce reactive sites (hydroxyl groups) on the surface that are amenable to attachment of similar chlorosilane-based initiators. Furthermore, to accurately apply our buckling-based metrology to polymer brushes supported on PDMS, the synthetic strategy for surface modification of PDMS and subsequent polymerization must satisfy the following criteria: (1) the brush/PDMS interface is sharp and can be described by a simple two-layer model, (2) the surface remains flat in the unwrinkled state so as to allow thickness measurements of the brush via ellipsometry, and (3) the polymer brush film is relatively defect-free.

The most prevalent method for introducing hydroxyl groups to the surface of PDMS is dry oxidation of the surface via exposure to either ultraviolet ozone (UV ozone) or oxygen plasma. Plasma oxidation is an extremely efficient process requiring short exposure times (typically less than a minute) but leads to a highly brittle silica-like surface of a few nanometers thickness that can display surface cracking due to densification.^{17,18} On the other hand, UV ozone treatment requires much longer exposure times (tens of minutes) and has been shown to generate a thick, porous, and brittle silicate-like layer^{19–22} of ill-defined thickness and

(13) Nolte, A. J.; Rubner, M. F.; Cohen, R. E. *Macromolecules* **2005**, *38*, 5367.

(14) Brandup, J.; Immergut, E. H.; Grulke, E. A. *Polymer Handbook*; Wiley-Interscience: New York, 1999.

(15) Caykara, T.; Ozyurek, C.; Kantoglu, M.; Erdogan, B. *Polym. Degrad. Stab.* **2003**, *80*, 339.

(16) Stafford, C. M.; Roskov, K. E.; Epps, T. H.; Fasolka, M. J. *Rev. Sci. Instrum.* **2006**, *77*, 023908.

(17) Owen, M. J.; Smith, P. J. *J. Adhes. Sci. Technol.* **1994**, *8*, 1063.

(18) Hillborg, H.; Ankner, J. F.; Gedde, U. W.; Smith, G. D.; Yasuda, H. K.; Wikstrom, K. *Polymer* **2000**, *41*, 6851.

(19) Ouyang, M.; Yuan, C.; Muisener, R. J.; Boulares, A.; Koberstein, J. T. *Chem. Mater.* **2000**, *12*, 1591.

(20) Efimenko, K.; Wallace, W. E.; Genzer, J. *J. Colloid Interface Sci.* **2002**, *254*, 306.

(21) Hillborg, H.; Tomczak, N.; Olah, A.; Schonherr, H.; Vancso, G. J. *Langmuir* **2004**, *20*, 785.

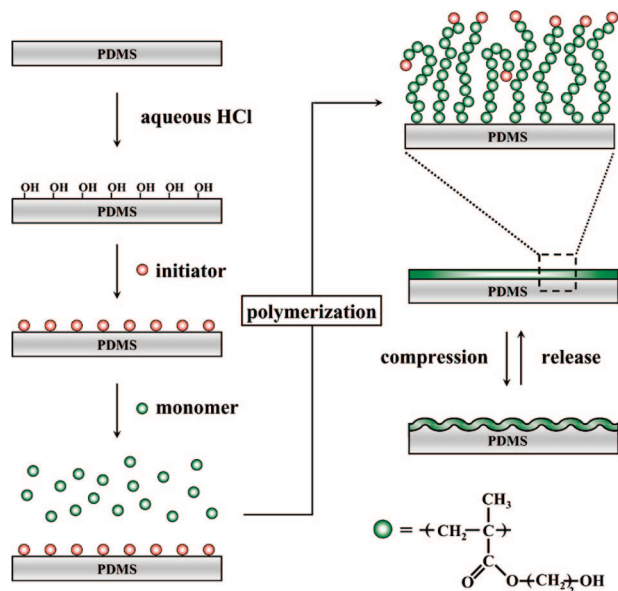


Figure 1. Illustration of the surface modification of PDMS by surface-initiated polymerization, forming a polymer brush layer that extends away from the interface, which can undergo surface wrinkling brought about by either mechanical or thermal compression.

modulus. Thus, surface modification by either UV-ozone or plasma oxidation fails to satisfy a number of our criteria for employing the buckling-based metrology to elucidate the properties of the polymer brush layer.

In contrast, we found that acid immersion consistently results in smoother surfaces that are optically transparent and lack noticeable defects when examined under an optical microscope, even under applied tensile and compressive strains. The advancing (θ_A) and receding (θ_R) water contact angles of HCl-treated PDMS were $\theta_A = 91.0 \pm 2.2^\circ$ and $\theta_R = 29.8 \pm 2.4^\circ$ compared to pristine PDMS, which showed contact angles of $\theta_A = 113.4 \pm 0.8^\circ$ and $\theta_R = 86.7 \pm 2.2^\circ$. The increase in surface energy of HCl-treated PDMS arises from the acid-induced cleavage of Si–O bonds along the PDMS chains, which leads to the formation of hydroxyl groups on the surface.^{23,24} Because of the hydrophobic nature of PDMS, the acid-induced cleavage is confined to the surface region of the PDMS, ensuring that the resulting polymer brush is restricted to the interface. Moreover, ATRP was conducted using a monomer mixture (HEMA in water) that does not swell PDMS, ensuring that the polymer chains would propagate from the initiator sites on the PDMS surface into the solution phase.

For our polymer brush layer, we chose to work with PHEMA due to both its amenability to the atom-transfer radical polymerization (ATRP) process and its wide interest for biomaterial applications ranging from drug delivery²⁵ to prosthetics.²⁶ The scheme for synthesizing PDMS-*g*-PHEMA brushes is graphically outlined in Figure 1 (see the Experi-

mental Section for details). Briefly, a silane-based initiator was subsequently reacted with the acid-treated PDMS. Polymerization progressed by exposing the PDMS with the bound surface initiator to a HEMA monomer solution. The brush thickness was tuned by varying the amount of time the PDMS was in contact with the monomer solution; thus, discrete brush thickness gradients could be created on a long PDMS substrate housed in a test tube by pumping in monomer solution in discrete steps. The presence of a discrete brush thickness gradient on a single piece of PDMS allowed us to employ a combinatorial approach to analyze the polymer brush layer and to reduce experimental uncertainty associated with the measurements.

Following ATRP on acid-treated substrates, the FTIR spectrum of the PDMS-*g*-PHEMA surface displayed the characteristic peaks of PHEMA at $\approx 3360 \text{ cm}^{-1}$ for the stretching vibration of the hydroxyl group and at $\approx 1730 \text{ cm}^{-1}$ for the stretching vibration of the carbonyl group. The static contact angle of the PDMS-*g*-PHEMA was nearly constant ($52.6 \pm 0.9^\circ$) along the thickness gradient, indicating the chemical homogeneity of the PHEMA brush. For comparison, the static contact angle of an untethered PHEMA film deposited onto a silicon wafer was $52.9 \pm 1.0^\circ$.

Ellipsometry is one of the most convenient tools to monitor the progress of polymer brush synthesis on inorganic substrates such as silicon or gold. However, as far as we are aware, there are no published reports where ellipsometry is used to measure the thickness of polymer brush layer on a transparent substrate such as PDMS. Recently, Nolte et al.^{13,27} demonstrated that variable angle spectroscopic ellipsometry (VASE) has the capability of measuring the thickness of a film of polyelectrolyte multilayers on PDMS. In our work, the uniformity and the high density of the polymer chains grafted from the HCl-treated PDMS surface enables the brush layer's refractive index (n) and thickness to be measured using VASE. The data indicate that the refractive index of PHEMA brushes ($n = 1.487 \pm 0.007$ at a wavelength of 633 nm) on PDMS is similar to that of solution-deposited PHEMA film on PDMS ($n = 1.493 \pm 0.005$). The brush thickness measured by ellipsometry increases linearly with the reaction time at a growth rate of $\approx 0.7 \text{ nm/min}$, which is similar to the growth rate on silicon as well as values reported previously in the literature.^{12,14}

3.2. Mechanical Wrinkling of Polymer Brushes. The mechanical properties of PHEMA brushes were assessed using a recently introduced buckling-based metrology^{28,29} that has been successfully employed on a number of different thin film systems.^{13,27,30–35} A characteristic wrinkling wavelength (λ) emerges on the surface of a thin, stiff film

- (22) Ye, H.; Gu, Z.; Gracias, D. H. *Langmuir* **2006**, *22*, 1863.
 (23) Perutz, S.; Kramer, E. J.; Baney, J.; Hui, C. Y. *Macromolecules* **1997**, *30*, 7964.
 (24) Perutz, S.; Wang, J.; Kramer, E. J.; Ober, C. K.; Ellis, K. *Macromolecules* **1998**, *31*, 4272.
 (25) Guiseppi-Elie, A.; Brahim, S. I.; Narinesingh, D. *Adv. Mater.* **2002**, *14*, 743.
 (26) Chirila, T. V. *Biomaterials* **2001**, *22*, 3311.

- (27) Nolte, A. J.; Cohen, R. E.; Rubner, M. F. *Macromolecules* **2006**, *39*, 4841.
 (28) Stafford, C. M.; Harrison, C.; Beers, K. L.; Karim, A.; Amis, E. J.; Vanlandingham, M. R.; Kim, H. C.; Volksen, W.; Miller, R. D.; Simonyi, E. E. *Nat. Mater.* **2004**, *3*, 545.
 (29) Stafford, C. M.; Guo, S.; Harrison, C.; Chiang, M. Y. M. *Rev. Sci. Instrum.* **2005**, *76*, 062207.
 (30) Mathur, A.; Erlebacher, J. *Appl. Phys. Lett.* **2007**, *90*, 061910.
 (31) Hendricks, T. R.; Lee, I. *Nano Lett.* **2007**, *7*, 372.
 (32) Watanabe, H.; Ohzono, T.; Kunitake, T. *Macromolecules* **2007**, *40*, 1369.
 (33) Lu, C. H.; Donch, I.; Nolte, M.; Fery, A. *Chem. Mater.* **2006**, *18*, 6204.

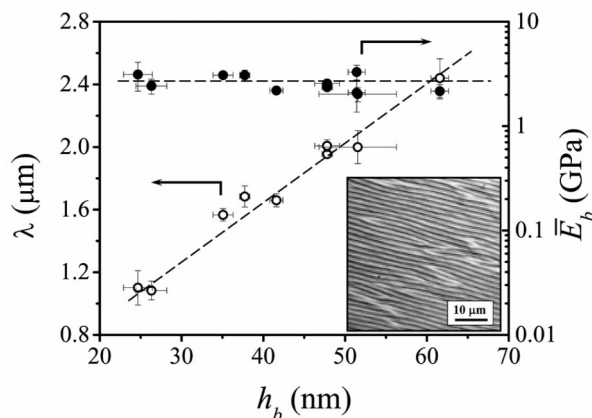


Figure 2. Mechanical wrinkling of PDMS-*g*-PHEMA along a thickness gradient. The wavelength (λ) of the wrinkles, as measured by optical microscopy (see inset), increases linearly with thickness in agreement with eq 1, resulting in a constant plane-strain modulus, $\bar{E}_b = 2.9 \pm 0.6$ GPa. Assuming $\nu_b = 0.33$, the Young's modulus of the brush layer is $E_b = 2.6 \pm 0.5$ GPa. The dashed lines are meant to guide the eye. The error bars represent one standard deviation of the data, which is taken as the experimental uncertainty of the measurement.

undergoing planar compression on a thicker, compliant substrate. The wavelength of the wrinkling pattern depends on the thickness of the film as well as the mechanical properties of the film and substrate as^{36,37}

$$\lambda = 2\pi h_b \left(\frac{\bar{E}_b}{3\bar{E}_s} \right)^{1/3} \quad (1)$$

where \bar{E} is the plane-strain modulus, defined as $E/(1 - \nu^2)$. E is the Young's modulus, h is the thickness, and ν is the Poisson's ratio. The subscripts b and s refer to the brush film and substrate, respectively. Equation 1 can be rearranged to solve for the modulus of the thin brush layer:

$$\bar{E}_b = 3\bar{E}_s \left(\frac{\lambda}{2\pi h_b} \right)^3 \quad (2)$$

By measuring the wrinkling wavelength, film thickness, and substrate modulus, the Young's modulus of the film can be determined using eq 2. By incorporating a gradient in brush thickness along the length of a single PDMS strip, we can conduct several measurements of the mechanical response of the brush under identical processing and environmental conditions. By constructing multiple gradient specimens with different ranges of thickness, we can survey a large parameter space of brush thickness while also incorporating replicate data points to ensure that minor differences in processing and/or environmental conditions between samples do not affect our measurements.

Figure 2 shows a compilation of wrinkling wavelength as a function of brush thickness as well as the brush modulus calculated using eq 2. The inset in Figure 2 is an optical micrograph of one region along the thickness gradient showing the wrinkling pattern. The wrinkles align perpendicular to the applied compressive strain. The wrinkling

wavelength increases linearly with the brush thickness, indicating that the Young's modulus of the PHEMA brush does not significantly depend upon thickness for the thickness regime studied in this work (25–65 nm). The average plane-strain modulus of the grafted PHEMA brush layers was found (via eq 2) to be $\bar{E}_b = 2.9 \pm 0.6$ GPa. Assuming a Poisson's ratio for the brush layer of $\nu_b = 0.33$, the average Young's modulus of the polymer brush is $E_b = 2.6 \pm 0.5$ GPa, comparable to a flow-coated PHEMA film ($E = 1.9 \pm 0.4$ GPa) measured by surface wrinkling. Both of these values for the modulus of PHEMA are in agreement with literature values ($E \approx 2$ GPa) reported for bulk PHEMA at room temperature.³⁸ In general, our results agree with the findings of Urayama et al.,³⁹ who reported modulus values for poly(methyl methacrylate) brush layers that are similar to the corresponding bulk polymer when measured using electromechanical interferometry. In contrast, Julthongpiput et al.⁴⁰ reported a Young's modulus of polystyrene brushes (measured using AFM) significantly less than the bulk value; however, the brush layers in that particular study were particularly thin ($h_b \approx 7$ nm). The inconsistency between the two studies might be attributed to the methods of the brush fabrication as well as the limitations of the models used in the studies. Van Vliet and co-workers recently reported that nanoindentation disturbs the interfacial structure of a polymer film and introduces artifacts in the measurement of mechanical properties of thin films, making such measurements difficult.^{11,41}

Conversely, we can also use surface wrinkling to measure the thickness of polymer brush layers grafted from PDMS. Although the thickness values of the PDMS-*g*-PHEMA samples in this study were measured by spectroscopic ellipsometry, VASE requires not only access to such an instrument but also a relatively large, flat sample (≈ 2 mm \times 2 mm) to gain enough signal resolution. In many practical applications of polymer brushes, such as microfluidic devices, the surface geometry is often irregular and complex, precluding the use of ellipsometry and many other common characterization techniques. A simple rearrangement of eq 2 shows that the film thickness is linearly proportional to the wrinkling wavelength if the mechanical properties of the film and substrate are assumed to remain constant:

$$h_b = \frac{\lambda}{2\pi} \left(\frac{\bar{E}_b}{3\bar{E}_s} \right)^{-1/3} \quad (3)$$

Since the modulus of a glassy polymer brush layer is normally several orders of magnitude higher than that of PDMS, a brush with a thickness on the order of tens of nanometers (difficult to measure directly) generates a wrinkling wavelength on the micron scale, which is readily measured using straightforward techniques such as optical microscopy and static light scattering.²⁹ Quantitative mea-

(34) Stafford, C. M.; Vogt, B. D.; Harrison, C.; Julthongpiput, D.; Huang, R. *Macromolecules* **2006**, *39*, 5095.

(35) Wilder, E. A.; Guo, S.; Lin-Gibson, S.; Faselka, M. J.; Stafford, C. M. *Macromolecules* **2006**, *39*, 4138.

(36) Huang, R. *J. Mech. Phys. Solids* **2005**, *53*, 63.

(37) Groenewald, J. *Physica A* **2001**, *298*, 32.

(38) Tobolsky, A. V.; Shen, M. C. *J. Phys. Chem.* **1963**, *67*, 1886.

(39) Urayama, K.; Yamamoto, S.; Tsujii, Y.; Fukuda, T.; Neher, D. *Macromolecules* **2002**, *35*, 9459.

(40) Julthongpiput, D.; LeMieux, A.; Tsukruk, V. V. *Polymer* **2003**, *44*, 4557.

(41) Thompson, M. T.; Berg, M. C.; Tobias, I. S.; Rubner, M. F.; Van Vliet, K. J. *Biomaterials* **2005**, *26*, 6836.

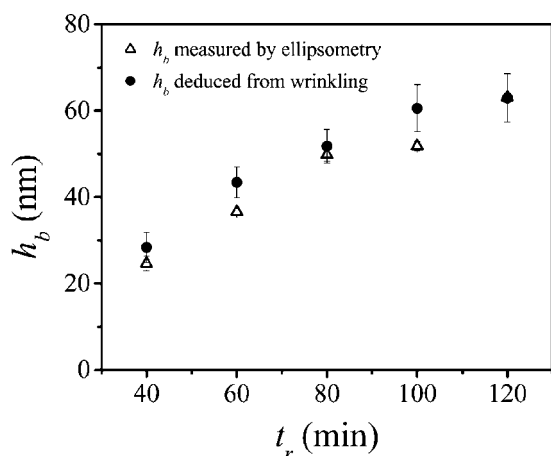


Figure 3. Brush thickness (h_b) both measured by ellipsometry (open triangles) and deduced from wrinkling (filled circles) versus reaction time (t_r) for forming a PHEMA brush thickness gradient on PDMS via ATRP. Wrinkling was induced by mechanical compression, and eq 3 was used to calculate the film thickness assuming $E_b = 1.9$ GPa and $\nu_b = 0.33$ for PHEMA. The two methods for determining film thickness are in excellent agreement, indicating that surface wrinkling can indeed provide an accurate measure of brush thickness without the need for specialized instruments.

measurements of the film thickness using eq 3 require the Young's modulus of the polymer brush to be known in advance. We demonstrate the effectiveness of this approach by comparing thickness values measured using eq 3 to those measured independently by spectroscopic ellipsometry. For this demonstration, we assume the brush modulus to be the same as a PHEMA film (i.e., $E_b = 1.9$ GPa). The results shown in Figure 3 suggest that surface wrinkling can quantitatively monitor the growth (e.g., thickness) of polymer brush layers on PDMS surfaces by simple measurement of the wrinkling wavelength under an optical microscope. Additionally, the film thickness is less sensitive to a small variation in the mechanical properties of the film due to the weak ($1/3$ power) dependence, making the estimated Young's modulus a relatively smaller source of error in this calculation.

3.3. Reversible Surface Wrinkling. In addition to mechanical compression, wrinkling can also be induced by heating a sample above its glass transition temperature (T_g) and cooling it back to room temperature.^{31,42} Upon heating, both the PDMS and polymer brush layer expand according to each material's coefficient of thermal expansion (α_s and α_b , respectively). However, at temperatures above the T_g of the polymer brush ($T_g \approx 85$ °C), the polymer chains in the brush layer can relax the thermal stress. Upon cooling, the polymer film becomes glassy below its T_g while the PDMS continues to contract, placing the film under compressive stress and inducing surface wrinkling. AFM images of thermally wrinkled patterns from a discrete thickness gradient of PDMS-*g*-PHEMA are shown in Figure 4a. The wrinkled patterns appear randomly oriented rather than aligned due to the isotropic stress induced by thermal treatment. In this case, wrinkling occurs at a critical temperature (T_c) that is about 10–20 °C below the T_g of the polymer brush. This critical temperature is directly related to the critical strain needed to induce wrinkling via $\epsilon_c \approx (\alpha_s - \alpha_b)(T_c - T_g)$. Once

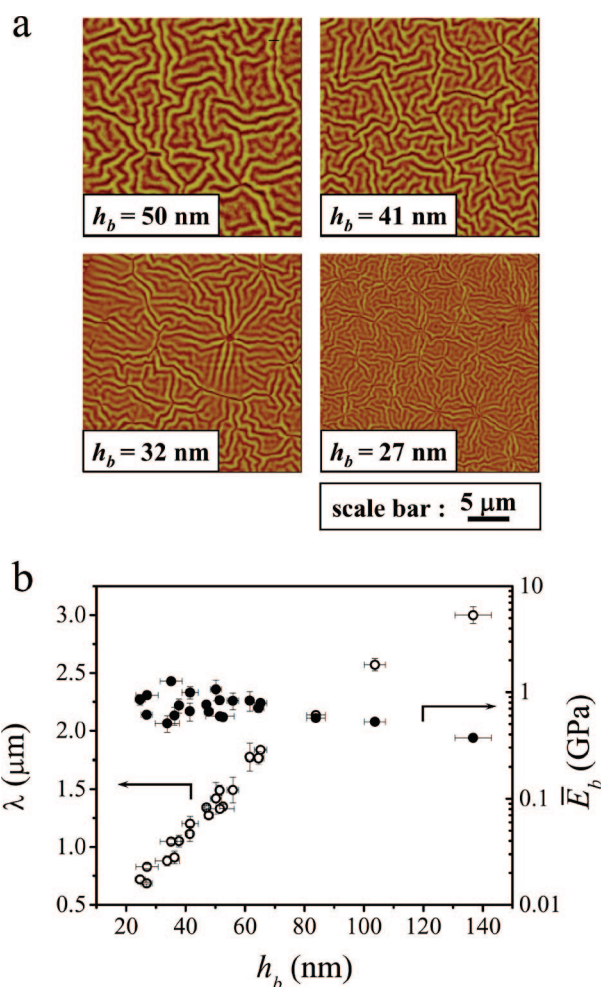


Figure 4. Thermal wrinkling of PDMS-*g*-PHEMA possessing a thickness gradient. (a) AFM height images of different zones of a PHEMA brush thickness gradient on PDMS. The patterns are randomly oriented due to the isotropic nature of the thermally induced stress. (b) Wrinkling wavelength (λ) and plane-strain modulus (E_b) as a function of brush thickness. The data are a collection of multiple overlapping thickness gradient samples, which allows for a wider parameter space to be probed with replicates. In this case, wrinkling occurs at some critical temperature (T_c), which can be directly related to the critical strain needed to induce wrinkling. Therefore, the measured modulus reflects the modulus of the brush layer at this critical temperature rather than the room temperature modulus probed in the case of mechanical compression.

the wrinkling pattern is formed, the wrinkling wavelength remains constant as the temperature decreases further, which is consistent with recent observations on thermally induced wrinkling of polystyrene–PDMS system.⁴³ Furthermore, this result parallels previous findings with the mechanically induced buckling that the wrinkling wavelength is insensitive to the magnitude of the compressive strain.⁴⁴ Thus, the Young's modulus derived from the thermally wrinkled pattern represents the modulus at T_c and is lower than the value measured by compression-induced wrinkling at room temperature.

Figure 4b illustrates the linear relationship between the wavelength of the thermally induced wrinkling pattern and the brush thickness for four individual gradient PDMS-*g*-PHEMA samples with thicknesses ranging from 25 to 140

(42) Mei, H. X.; Huang, R.; Chung, J. Y.; Stafford, C. M.; Yu, H. H. *Appl. Phys. Lett.* **2007**, *90*, 151902.

(43) Chung, J. Y.; Stafford, C. M. Unpublished data.

(44) Chung, J. Y.; Youngblood, J. P.; Stafford, C. M. *Soft Matter* **2007**, *3*, 1163.

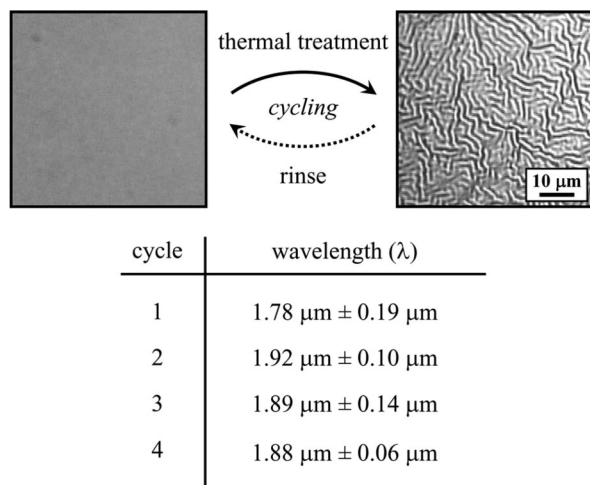


Figure 5. Thermal wrinkling of PDMS-*g*-PHEMA, which can be reversed or “erased” by rinsing with a good solvent for the PHEMA (e.g., water, ethanol, DMF). Thermal treatment (heating above the T_g of the brush) leads to surface wrinkling upon cooling, and the wrinkles remain until rinsed with a fluid such as water that swells and relaxes the PHEMA brush but does not swell the underlying PDMS substrate. One cycle of thermal treatment/rinsing (wrinkled/flat) is shown in the optical micrographs (top). The wavelength of the wrinkling pattern ($h_b = 65$ nm) remains reasonably constant after several cycles of thermal treatment and rinsing, as shown in the table (bottom).

nm. The resulting Young’s modulus was found to be fairly constant with film thickness, with an average value of $E_b = 0.72 \pm 0.17$ GPa. For comparison, we used thermal wrinkling to measure the Young’s modulus of a flow-coated PHEMA film ($h \approx 50$ nm) on PDMS and found the modulus ($E = 0.64 \pm 0.07$ GPa) to be quite similar. Both results are comparable to literature values for the Young’s modulus of PHEMA at 75 °C ($E \approx 0.5$ GPa).³⁸

One of the most salient features of polymer brush wrinkling lies in its reversibility in response to alternating solvent and thermal treatments. Because it is covalently bound to the PDMS, exposure of the polymer brush layer to a good solvent does not remove it from the surface but rather allows the chains to relax and release any strain energy stored in the system, leading to a reflattening of the surface if it had been previously wrinkled. Figure 5 shows optical microscopy images of a PDMS-*g*-PHEMA sample during one cycles of thermal and solvent treatment. As mentioned

above, the thermal treatment results in the formation of an isotropic wrinkled pattern, while the treatment of the sample with a solvent (e.g., DMF or methanol), which favors PHEMA but is not compatible with PDMS, swells the polymer brush, and erases the wrinkled pattern, leading to a flat surface upon drying. Therefore, the wrinkled pattern can be switched on and off via a repetitive cycle of thermal and solvent treatment. The ability to create reversible surface patterns may have potential uses for many applications, including the controllable adjustment of surface texture and roughness to affect interfacial adhesion, the tuning of the optical scattering properties of a surface, and the introduction of patterns into the channels of microfluidic devices to reversibly control flow patterns.

4. Conclusions

In summary, we have demonstrated that surface wrinkling is an effective tool for measuring both the Young’s modulus as well as the thickness of polymer brushes grafted from PDMS. Both mechanically and thermally induced wrinkling patterns suggest that the Young’s modulus of a PHEMA brush layer is relatively insensitive to film thickness over the thickness range tested in this paper and has a numerical value similar to the reported bulk value. Wrinkled patterns can be repeatedly induced and erased via thermal and solvent treatment, thus manifesting a switchable surface texture. Our results serve to broaden the applicability of surface wrinkling as an important metrology tool for the field of surface science and offer a new route toward responsive surface patterning, which can be used in fields such as adhesion and microfluidics, where both surface chemistry and surface morphology play a key role in governing performance.

Acknowledgment. The authors thank Drs. K. L. Beers and C. Xu for help with ATRP, Dr. L. J. Richter for help with spectroscopic ellipsometry, and Dr. K. T. Tan for the operation of ATR-FTIR. The authors also thank Drs. M. J. Fasolka and M. L. Becker for critically reading the manuscript. This work was conducted at the NIST Combinatorial Methods Center. A. J. N. gratefully acknowledges the NIST/NRC Postdoctoral Fellowship Program for funding.

CM702456U